HIERARCHICAL ZEOLITES MODIFIED WITH CHITOSAN – SYNTHESIS AND CHARACTERISATION

Agnieszka Feliczak-Guzik[a], [*], Ewelina Musielak[b], Izabela Nowak[c]

Adam Mickiewicz University, Faculty of Chemistry, Uniwersytetu Poznańskiego 8, 61-614 Poznań, Poland
[a] - ORCID: 0000-0002-1875-5415; [b]- ORCID: 0000-0003-0683-4631; [c] - ORCID: 0000-0002-1113-9011

** corresponding author: agaguzik@amu.edu.pl*

Abstract

This paper describes the synthesis of hierarchical zeolites based on a commercial FAU zeolite modified with chitosan. Additionally, the amount of silicon source added (tetraethyl orthosilicate) and the type of structuring agent used were modified during synthesis of the materials. The synthesised materials were characterised by the following methods: X-ray diffraction, transmission electron microscopy, scanning electron microscopy, Fourier-transform infrared spectroscopy, and low-temperature nitrogen adsorption/desorption isotherms. The obtained results confirmed the achievement of additional porosity in the synthesised materials. According to the adsorption experiments, the hierarchical zeolite-modified chitosan had a high adsorption capacity of 1.2 $cm^3\ g^{-1}$.

Keywords: *hierarchical zeolites, chitosan, secondary porosity, methods for characterising porous materials*

Received: 28.02.2022
Accepted: 26.05.2022

1. Introduction

Zeolites are crystalline aluminosilicates with the general formula $M_{x/n}[Al_xSi_yO_{2(x+y)}]\cdot zH_2O$, where M represents cations with charge n (+1 and/or +2), y/x = 1 – 5, and z/x = 1 – 4. They are classified as microporous materials with a pore size <2 nm according to the International Union of Pure and Applied Chemistry (IUPAC) classification and are characterised, among other things, by the presence of strong acid centres, a well-defined pore system, and a large specific surface area. Their main disadvantage is that these materials exhibit diffusion limitations for more branched molecules and the transport of reactants with sizes close to the diameter of the micropores is hindered; hence, only the outer part of the zeolite grain is involved in the catalytic reaction and its interior is catalytically inactive. These deficiencies can be eliminated by using so-called hierarchical zeolites, characterised by the presence of secondary porosity – that is, the presence of at least one additional pore system, mainly in the mesopore range from 2 to 50 nm according to IUPAC classification. Compared with classical zeolites, the use of hierarchical zeolites as catalysts for catalytic reactions can increase the catalytic activity and decrease the susceptibility of the catalyst to deactivation [1-3]. Additionally, compared with microporous zeolites these materials, eliminate diffusion limitations for larger and branched particles with sizes close to the diameter of the micropores [4]. There are several procedures to prepare hierarchical materials including, but not limited to, the use of zeolite seeds, hard/soft templating, or dealumination or desilication [5, 6].

Declining renewable resources and increasing environmental concerns have led to a paradigm shift in the use of available resources. Biomass valorisation has recently received considerable attention as an attempt to produce high-value chemicals. Interest in using biomass-derived polymeric materials (e.g., cellulose, lignin, and chitin) to synthesise carbon-based catalysts continues to grow. These materials are non-toxic, biodegradable, and biocompatible [7, 8]. Chitin is a straight-chain biopolymer that is the second most abundant polysaccharide on Earth after cellulose. It is the building block of the exoskeleton of marine animals such as crabs, shrimp, and lobsters [9]. Despite the fact that approximately 6-8 million tons of chitin waste are produced annually worldwide, the potential value of chitin waste to the chemical and materials industries is largely overlooked [10]. Chitin is a relatively underused compound due to its insolubility in common solvents and expensive and uneconomical methods of extracting chemicals from it. These factors limit its use in various industrial fields, although it is used in biomedicine, food technology, and textiles [11]. Chitosan is a natural biopolymer obtained by partial *N*-deacetylation of chitin. Various methods such as steam explosion, alkaline treatment, and enzymatic deacetylation are used to deacetylate chitin [12]. Highly concentrated alkaline treatment is the most widely used method for chitin deacetylation [13]. The characteristic properties of chitosan are mainly due to its high content of reactive amino and hydroxyl groups. It is used in medicine, pharmacy, biochemistry, food, cosmetics, and agriculture [14-16].

This paper presents the synthesis of hierarchical zeolites modified with chitosan and their physicochemical characterisation. The amount of silicon source added and the type of structuring agent were modified during optimisation of the synthesis conditions of the above-mentioned materials. In subsequent studies, we would like to evaluate the usefulness of these new materials for modifying the release profiles of active pharmaceutical ingredients.

2. Materials and Methods

2.1. Synthesis of Hierarchical Materials Modified With Chitosan

Chitosan-modified hierarchical zeolites were synthesised from a commercial faujasite (FAU)-type zeolite. The FAU zeolite (0.50 g), ethyl alcohol (60.00 g), ammonia water (1.25 g), structuring agent – non-ionic ones, including Brij S10 (polyethylene glycol octadecyl ether, $C_{18}H_{37}(OCH_2CH_2)_nOH$, n~10), and Lutrol F127 (generic name: poloxamer 407), or an ionic one, namely cetyltrimethylammonium bromide (CTABr, Fluka) – in the amount of 0.35 g, and distilled water (100.00 g) were combined. The mixture was treated with ultrasound at 65°C for 30 min. Then, the mixture was transferred to a magnetic stirrer with a heating function, where the silicon source tetraethyl orthosilicate (TEOS) in the amount of 0.28, 0.56, or 1.12 g and chitosan in the amount of 0.008 g were added during continuous stirring. The mixture was stirred for 4 h at 65°C. After the specified time, the mixture was removed from the magnetic stirrer and placed in a dryer for 24 h at 65°C. Then, the preparations were gravitationally filtered on a glass funnel by washing three times with a 1:1 mixture of distilled water and ethanol. After washing, the precipitate was left to dry for 24 h. The next step in the synthesis was the extraction of the zeolite material to remove the structuring agent. The process was carried out in a 100:1 mixture of ethanol and hydrochloric acid (HCl) (100 ml EtOH and 1 ml HCl). The prepared solutions were poured into glass bottles, placed on a magnetic stirrer, and the temperature was stabilised to 60°C. After normalising the solution temperature inside the containers, the mixture was stirred for 20 h on a magnetic stirrer.

2.2. Characteristics of the Obtained Materials

The resulting hierarchical materials were characterised using the following techniques:

- X-ray diffraction (XRD) in the low-angle range (SXRD) and the high-angle range (WXRD);
- Fourier-transform infrared (FT-IR) spectroscopy;
- Low-temperature nitrogen adsorption/desorption;
- elemental analysis;
- transmission electron microscopy (TEM); and
- scanning electron microscopy (SEM).

2.2.1. XRD

XRD was performed using a Bruker AXS D8 Advance diffractometer with a Johannson monochromator and a LynxEye strip detector. The CuKα radiation source generated a wavelength of 0.154 nm in the low-angle range of 2Θ = 0.6-8.0° (with 0.02° accuracy) and in the high-angle range of 2Θ = 6.0-60.0° (with 0.05° accuracy).

2.2.2. FT-IR

Spectroscopic studies were performed using an Agilent Technologies Cary 630 FT-IR spectrophotometer using the total reflection IR technique. All scans were made in the range of 4000-650 cm^{-1} with a resolution of 8 cm^{-1}.

2.2.3. Low-Temperature Isotherms of Nitrogen Adsorption/Desorption

Measurements were made using a Quantachrome Autosorb iQ instrument. Before performing the actual measurement, the tested samples were degassed under a vacuum at 110°C for 24 h. Isotherms were obtained at ca. -196°C. The Brunauer-Emmet-Teller (BET) specific surface area was determined by using the BET method. The pore volume was determined by using a modification of the Barrett-Joyner-Halenda (BJH) algorithm, the KJS-BJH method, while the external and mesoporous surface areas were determined by using the t-plot method.

2.2.4. Elemental Analysis

The elemental composition of the synthesised catalysts was determined by using the Elementar Analyser Vario EL III instrument. The method of measurement was based on catalytic combustion of a sample weight at 1200°C and analysis of the composition of gaseous products of combustion based on differences in their thermal conductivity.

2.2.5. TEM

Transmission electron micrographs were obtained using a JEOL-2000 microscope with an accelerating voltage of 80 kV.

2.2.6. SEM

Scanning electron micrographs were obtained using a Zeiss EVO type microscope. The analysed samples were bombarded with an electron beam of 17 kV energy. The resulting materials are named FAU_x_CHIT_y, where FAU refers to the type of zeolite, x refers to the type of template (BRIJ, LUTROL, or CTABr), CHIT refers to chitosan, and y is the amount of TEOS.

3. Results and Discussion

The diffractogram for the commercial FAU-type zeolite is presented in Figure 1A, while the low-angle diffractograms for the chitosan-modified hierarchical materials are shown in Figure 1B-D. A characteristic clear reflection at 2θ of ~2.5° indicates that an additional mesoporous structure in the materials prepared based on the ionic structuring agent. In the case of catalysts obtained with non-ionic structuring agents, the intensity of this reflex is insignificant.

On the other hand, wide-angle diffractograms of the synthesised materials (Figure 2B-D) confirm preservation of the crystalline structure of the commercial zeolite (Figure 2A). Additionally, there are no reflections characteristics of chitosan (2θ = 11.8° and 19.9°), corresponding to an amorphous chitosan structure due to the presence of signals from the FAU zeolite [17]. However, there is a slight increase in these signals when compared with the parent FAU diffractogram, suggesting that chitosan was intercalated into the surface of the hierarchical zeolite.

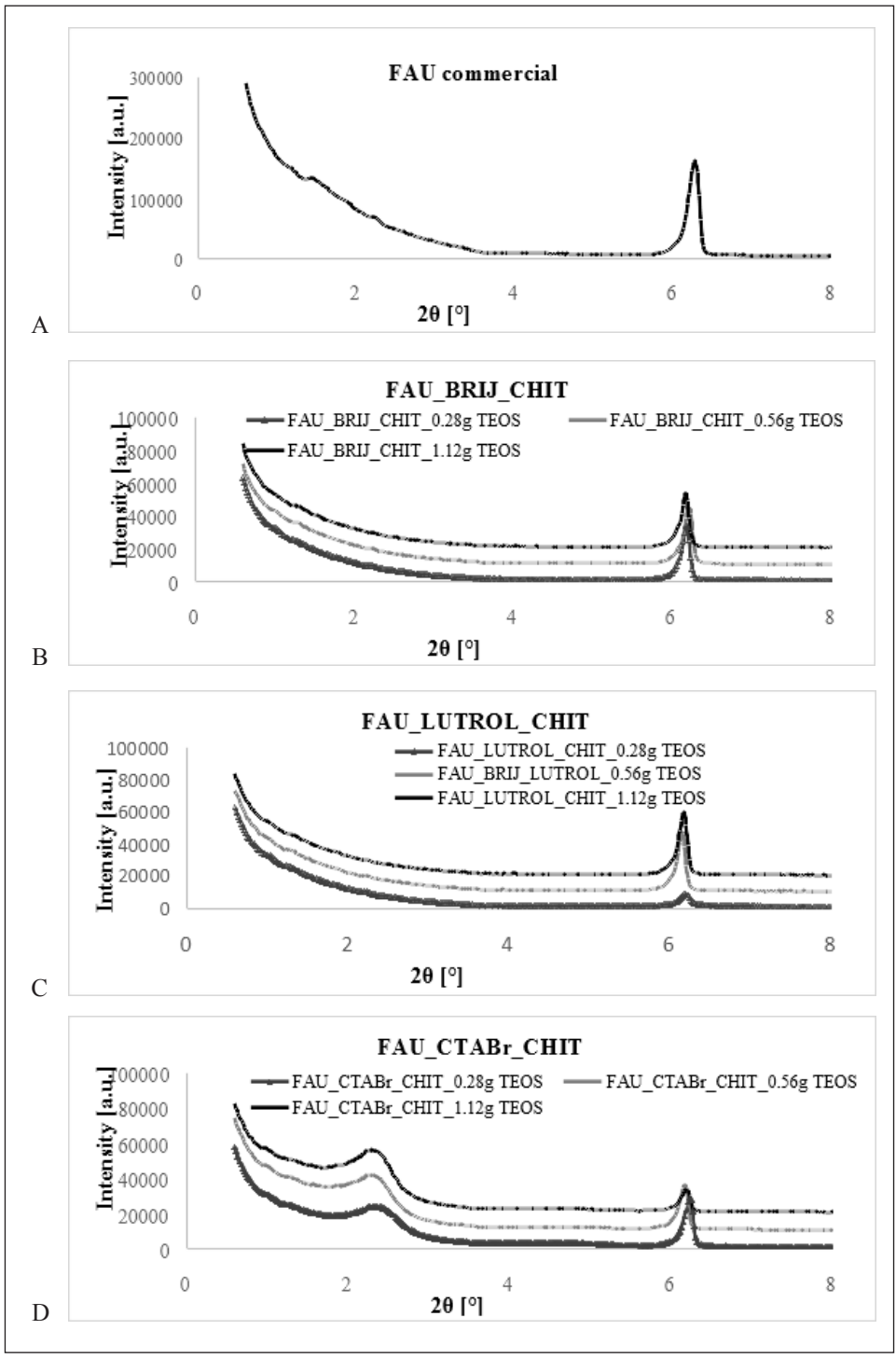

Figure 1. Low-angle X-ray diffraction patterns of prepared materials: commercial zeolite (A), FAU_BRIJ_CHIT (B), FAU_LUTROL_CHIT (C), and FAU_CTABr_CHIT (D). The diffractograms shifted by a constant value of 10000 contract units relative to the preceding diffractogram.

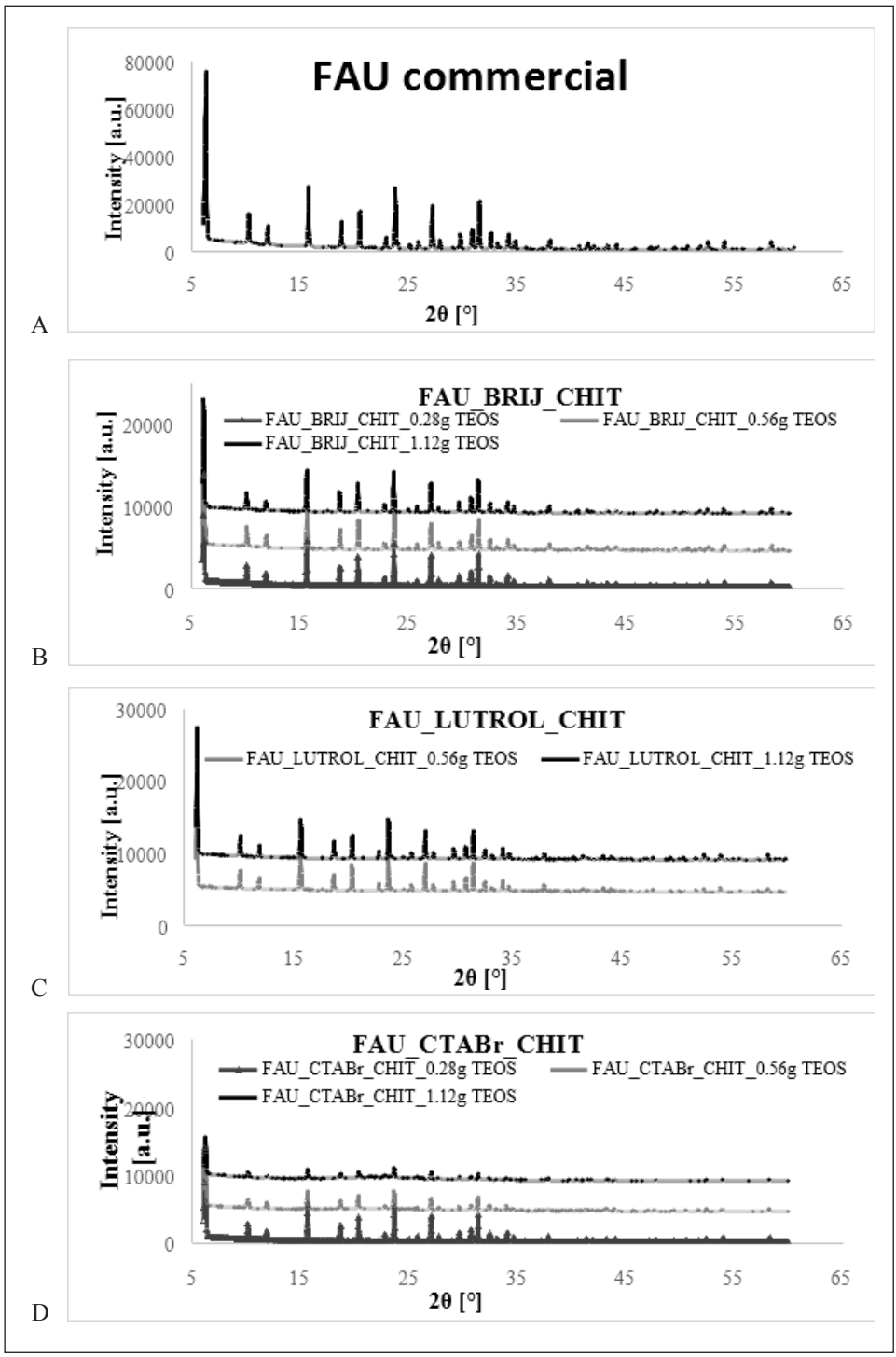

Figure 2. Wide-angle X-ray diffraction patterns of prepared materials: commercial zeolite (A), FAU_BRIJ_CHIT (B), FAU_LUTROL_CHIT (C), and AU_CTABr_CHIT (D). The diffractograms shifted by a constant value of 4500 contract units relative to the preceding diffractogram.

The efficiency of removing the surfactant from the pores of synthesised materials using an extraction process was evaluated. A commonly available technique used to verify surfactant removal from material pores is FT-IR spectroscopy. The bands in the spectrum of the hierarchical zeolites (Figure 3) that occur at ~2902, ~2857, and ~2863 cm^{-1}, can be attributed to the stretching vibrations of the $-CH_2$ and $-CH_3$ groups, originating from the surfactant. In contrast, the bands at ~1465-1440 cm^{-1} can be attributed to the asymmetric vibrations of the $-CH_2$ groups and the bands at 1410-1350 cm^{-1} and 1390-1370 cm^{-1} correspond to the bending

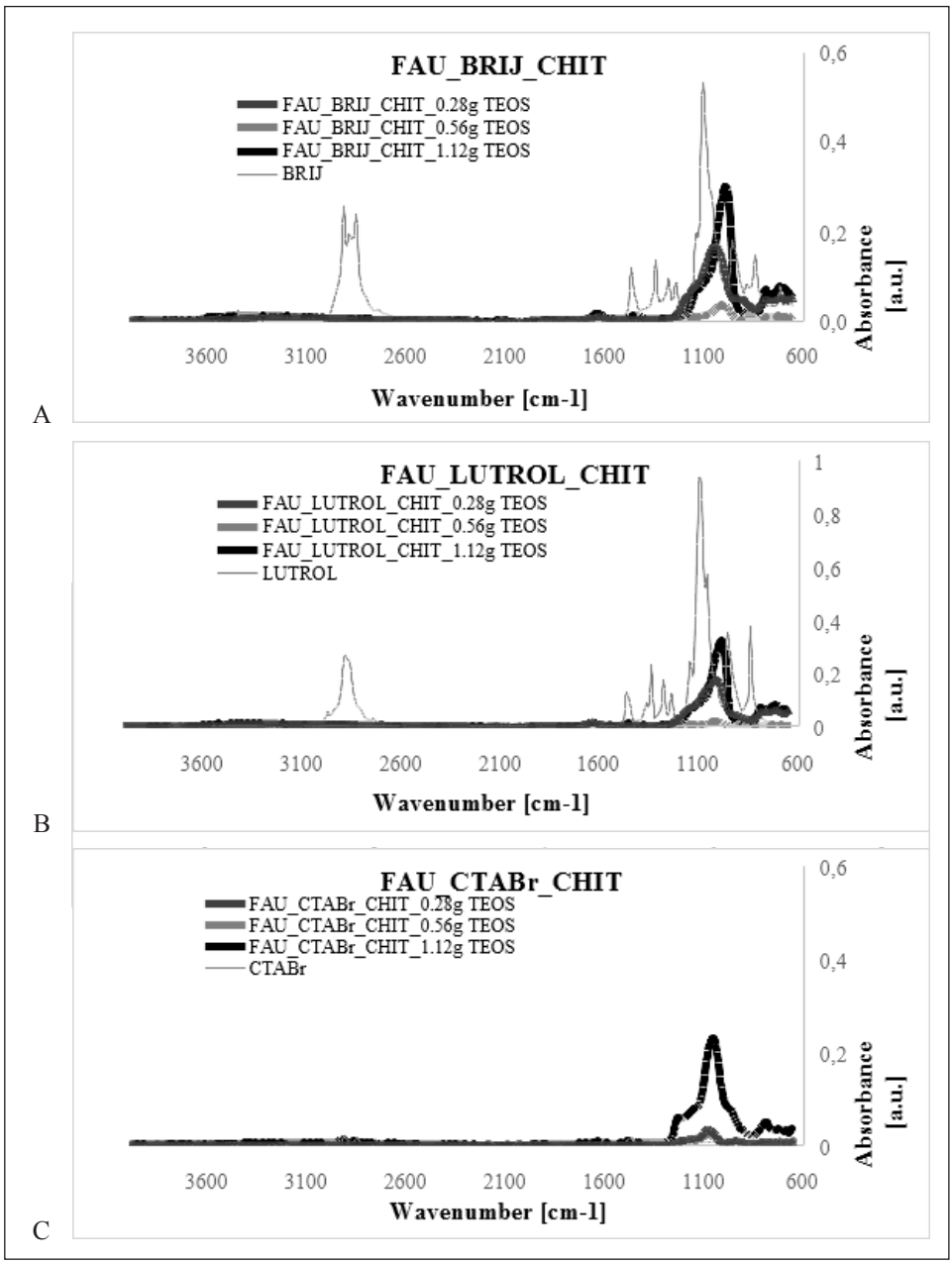

Figure 3. Fourier-transform infrared spectra of the synthesised materials: FAU_BRIJ_CHIT (A), FAU_LUTROL_CHIT (B), and FAU_CTABr_CHIT (C).

and symmetric vibrations of the -CH_3 group, respectively [18]. Only FAU_CTABr_CHIT_1.12 g TEOS shows these bands (Figure 3C). In the other materials, the structuring agent was removed efficiently. The band at about 1100 cm^{-1} indicates asymmetric stretching vibrations of Si-O-Si and that at about 800 cm^{-1} indicates symmetric stretching of the Si-O-Si bond. The bands at 960 cm^{-1} are attributed to the presence of silanol groups (Si-OH) [19].

Nitrogen adsorption/desorption isotherms for the synthesised materials are shown in Figure 4. The commercial FAU-type zeolite has a type I isotherm according to the IUPAC

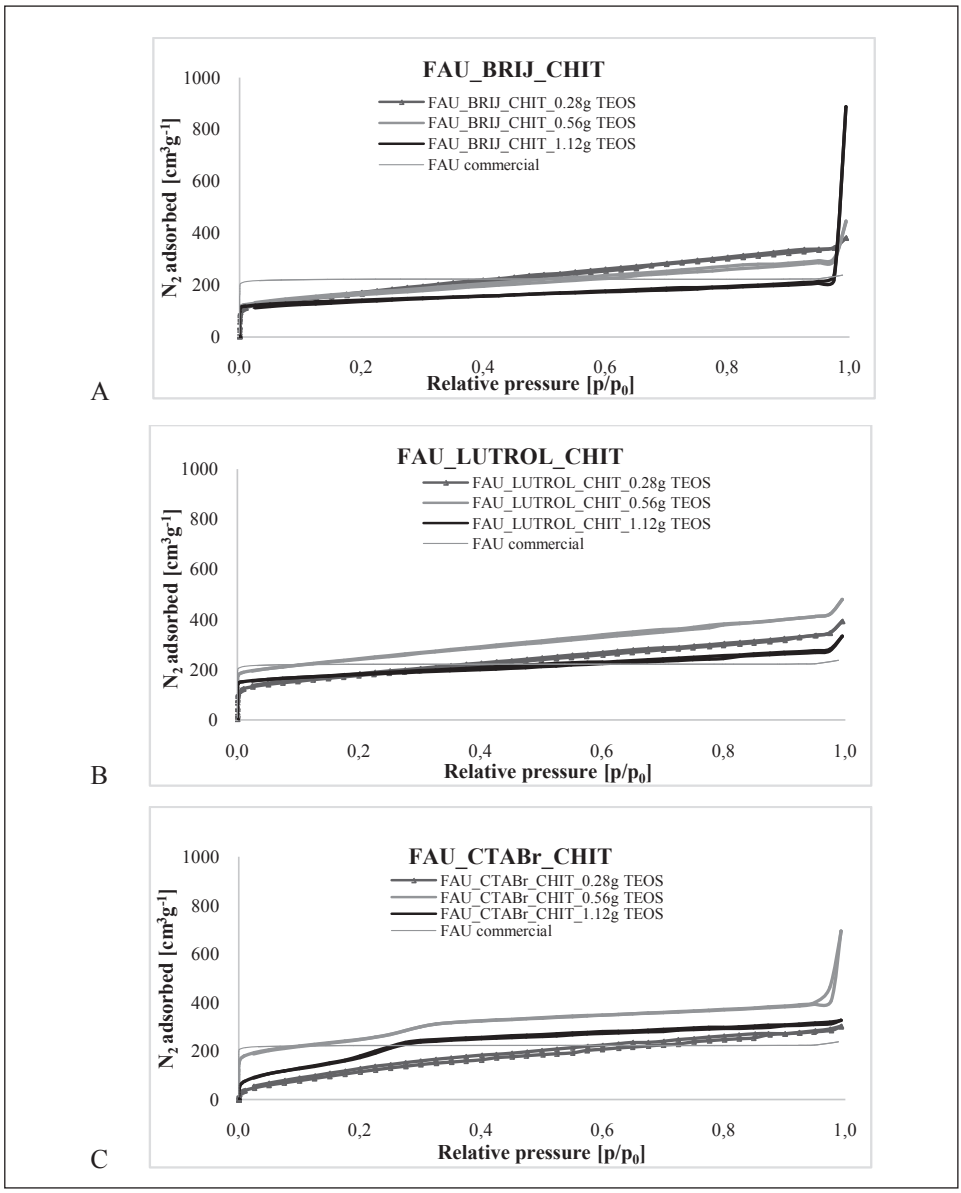

Figure 4. Isotherms of nitrogen adsorption/desorption for the materials based on the commercial FAU zeolite: FAU_BRIJ_CHIT (A), FAU_LUTROL_CHIT (B), and FAU_CTABr_CHIT (C).

classification, which is characteristic of microporous materials [20]. The other materials have a mixture of type I and IVa isotherms. Type IVa is characteristic of mesoporous materials. These results confirm the acquisition of additional secondary porosity in the synthesised materials. Moreover, depending on the type of structuring agent used and the amount of silicon source added during the synthesis, there is a slightly different increase in the total amount of adsorbed nitrogen, which may indicate an increase in textural properties. For materials modified in the high relative pressure region, there is a rapid increase in adsorbed nitrogen, indicating the formation of secondary porosity, called textural porosity [21, 22].

Textural properties for hierarchical materials based on commercial FAU-type zeolite are shown in Table 1.

Table 1. Porous structure parameters of the synthesised hierarchical zeolites.

Materials	Surface area [m^2/g]			Pore volume, BJH [cm^3/g]	Average pore size [nm] > 2 nm
	S_{BET}	S_{mikro} t-plot	S_{ext} t-plot		
FAU Commercial	720	690	30	0.05	Absent
FAU_BRIJ_CHIT_0.28g TEOS	590	400	190	0.35	2.81
FAU_BRIJ_CHIT_0.56g TEOS	540	390	150	0.48	2.97
FAU_BRIJ_CHIT_1.12g TEOS	440	360	80	1.20	2.92
FAU_LUTROL_CHIT_0.28g TEOS	610	450	150	0.38	3.31
FAU_LUTROL_CHIT_0.56g TEOS	800	620	180	0.405	2.91
FAU_LUTROL_CHIT_1.12g TEOS	560	440	130	0.26	2.98
FAU_CTABr_CHIT_0.28g TEOS	530	350	180	0.33	3.71
FAU_CTABr_CHIT_0.56g TEOS	920	800	120	0.65	3.14
FAU_CTABr_CHIT_1.12g TEOS	890	780	110	0.17	2.97

The specific surface area of the obtained materials was determined using the BET method. The specific surface area of S_{BET} compared with the commercial FAU-type zeolite increases only in the case of materials prepared with CTABr as a structuring agent and with addition of 0.56 or 1.12g of TEOS. In other cases, the surface area decreases, which may be due to pore blocking by the modifying agent (chitosan) [23, 24]. The pore volume distribution function was calculated using the BJH algorithm. All materials except commercial zeolite type FAU have a uniform pore size distribution in the mesopore range (Table 1). The outer and microporous surface areas were determined using the t-plot method. Compared with the commercial FAU-type zeolite, there was a significant increase in the microporous surface area and a concomitant decrease in the outer surface area of the synthesised materials. Based on the analysis of all the obtained results, the optimum parameters are obtained for the samples synthesised using CTABr as the structuring agent and 0.56 g of TEOS.

Elemental analysis (Table 2) was performed to quantify organic molecules on the surface of chitosan-modified hierarchical zeolites (for samples synthesised under optimal synthesis conditions, i.e., using CTABr and 0.56 g of TEOS). The modified materials (containing chitosan) showed higher concentrations of H and C compared with the commercial FAU-type zeolite. This confirms the presence of anchored functionalised groups on the surfaces of these materials. The FAU_CTABr_CHIT_0.56g TEOS sample contains 13 times more nitrogen than the commercial material.

Usually, Si-O-T in the zeolite molecular sieve and the hydroxyl group (O-H) in the chitosan are connected by hydrogen bonds. Therefore, O plays a major role in the connection of chitosan and zeolite molecular sieves. Such hydrogen bonding/electrostatic bonding is responsible for active substance adsorption/desorption [25]. Thus, FAU_CTABr_CHIT is expected to be a good support for the active phase of the drugs or removal of cations from water [26].

Table 2. Elemental analysis of the commercial FAU-type zeolite and the synthesised hierarchical materials.

Materials	% N	% C	% H	% S
FAU commercial	0.12	0.74	0.35	0.07
FAU_BRIJ_CHIT_0.56g TEOS	0.19	2.88	2.71	0.00
FAU_LUTROL_CHIT_0.56g TEOS	1.61	2.69	3.87	0.00
FAU_CTABr_CHIT_0.56g TEOS	1.68	2.19	4.13	0.00

Transmission electron micrographs of the chitosan-modified materials (Figure 5A) suggest the presence of chitosan particles on their surface. In contrast, Figure 5B shows scanning electron micrographs. Based on the SEM analysis, there are no changes in the morphology of the obtained materials compared with the commercial material. It is well known that the surface of chitosan presents a sheet structure and appears patchy in sections [27]. Thus, the surface of the synthesised hierarchical zeolite comprises particles with regular morphology and a uniform size, which conforms to the morphology of the zeolite and not chitosan.

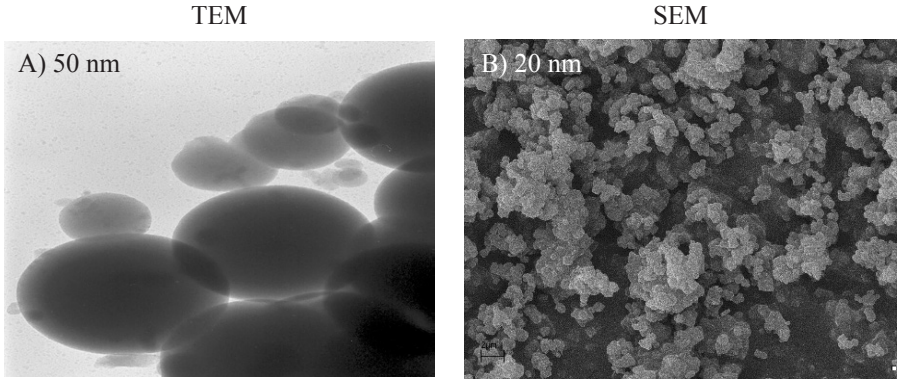

Figure 5. Transmission and electron micrographs of FAU_CTABr_CHIT_0.56g TEOS.

4. Conclusions

Chitosan-modified hierarchical materials have been successfully synthesised under different conditions, as confirmed by the results of physicochemical analyses. Based on these results, it was found that:

1. the synthesised materials had additional secondary porosity (in the mesoporous range), as confirmed by XRD (presence of reflections at 2θ ~1.5-2.5°) and low-temperature nitrogen adsorption/desorption isotherms (mixture of type I and IV isotherms);

2. the structure of the commercial FAU-type zeolite was preserved during most of the synthetic steps (high-angle diffractograms);
3. the obtained hierarchical materials had a high specific surface area, 440-920 m^2/g, and a homogeneous pore size distribution, with the average pore size varying from 2.8 to 3.7 nm.

Moreover, based on the analysis of all the obtained results, the optimal structure and texture parameters were obtained for the samples synthesised using CTABr as a structuring agent and 0.56 g of TEOS. The present work provides basic information that should be useful for future research on new mesoporous hierarchical zeolites used as potential carriers of active substances or the removal of pollutants from water.

5. Acknowledgments

A.F.-G. would like to acknowledge the project 'Excellence Initiative - Research University'- Competition No: 007, Support for the most scientifically productive young staff ('youth bonus'). E.M. would like to thank for the support from grant no. POWR.03.02.00-00-I020/17 co-financed by the European Union through the European Social Fund under the Operational Program Knowledge Education Development.

6. References

[1] Hartmann M, Gonche A, Schwieger W; (2016) Catalytic test reactions for the evaluation of hierarchical zeolites. Chem Soc Rev 45, 3313-3330. **DOI**:10.1039/C5CS00935A

[2] Chal R, Gérardin C, Bulut M, van Donk S; (2011) Overview and industrial assessment of synthesis strategies towards zeolites with mesopores. ChemCatChem 3, 67-81. **DOI**:10.1002/cctc.201000158

[3] Feliczak-Guzik A; (2018) Hierarchical zeolites: synthesis and catalytic properties. Microporous Mesoporous Mater 259, 33-45. **DOI**:10.1016/j.micromeso.2017.09.030

[4] Müller JM, Mesquita GC, Franco SM, Borges LD, deMacedo JL, Dias JA, Dias SCL; (2015) Solid-state dealumination of zeolites for use as catalysts in alcohol dehydration. Microporous Mesoporous Mater 204, 50-57. **DOI**:10.1016/j.micromeso.2014.11.002

[5] Koohsaryan E, Anbia M; (2016) Nanosized and hierarchical zeolites: a short review. Chin J Catal 37, 447-467. **DOI**:10.1016/S1872-2067(15)61038-5

[6] Karge HG, Weitkamp J (eds); (2002). Post-synthesis modification I. Springer-Verlag, Berlin.

[7] Varma RS; (2019) Biomass-derived renewable carbonaceous materials for sustainable chemical and environmental applications. ACS Sustainable Chem Eng 7, 6458-6470. **DOI**:10.1021/acssuschemeng.8b06550

[8] Zahedifar M, Es-Haghi A, Zhiani R, Sadeghzadeh SM; (2019) Synthesis of benzimidazolones by immobilized gold nanoparticles on chitosan extracted from shrimp shells supported on fibrous phosphosilicate. RSC Adv 9, 6494-6501. **DOI**:10.1039/C9RA00481E

[9] Jiang Z, Jiang ZJ, Tian X, Chen W; (2014) Amine-functionalized holey graphene as a highly active metal-free catalyst for the oxygen reduction reaction. J Mater Chem A 2, 441−450. **DOI**:10.1039/C3TA13832A

[10] Gao X, Chen X, Zhang J, Guo W, Jin F, Yan N; (2016) Transformation of chitin and waste shrimp shells into acetic acid and pyrrole. ACS Sustain Chem Eng 4, 3912-3920. **DOI**:10.1021/acssuschemeng.6b00767

[11] Yan N, Chen X; (2015) Sustainability: don't waste seafood waste. Nature 524, 155-157. **DOI**:10.1038/524155a.

[12] Sivashankari PR, Prabaharan M; (2017) Deacetylation modification techniques of chitin and chitosan. In: Jennings JA, Bumgardner JD (eds), Chitosan based biomaterials volume 1: fundamentals. Elsevier, Cambridge, 117-133. **DOI**:10.1016/C2014-0-03147- 4

[13] Paulino AT, Simionato JI, Garcia JC, Nozaki J; (2006) Characterization of chitosan and chitin produced from silkworm crysalides. Carbohydr Polym 64, 98-103. **DOI**:10.1016/j.carbpol.2005.10.032

[14] Nithya A, Kumari HLJ, Chandra Mohan S, Ruckmani K, Jothivenkatachalam K.; (2016) Physicochemical investigations of biogenic chitosan-silver nanocomposite as an antimicrobial and anticancer agent. Int J Biol Mac 92, 77-87. **DOI**:10.1016/j.ijbiomac.2016.07.003

[15] Youssef AM, Abdel-Aziz MS, El-Sayed SM; (2014) Chitosan nanocomposite films based on Ag-NP and Au-NP biosynthesis by Bacillus Subtilis as packaging materials. Int J Biol Mac 69, 185-191. **DOI**:10.1016/j.ijbiomac.2014.05.047

[16] Anitha A, Sowmya S, Sudheesh Kumar PT, Deepthi S, Chennazhi KP, Ehrlich H, Tsurkan M, Jayakumar R; (2014) Chitin and chitosan in selected biomedical applications. Prog Polym Sci 39, 1644-1667. **DOI**:10.1016/j.progpolymsci.2014.02.008

[17] Rhim JW, Hong SI, Park HM, Ng PKW; (2006) Preparation and characterization of chitosan-based nanocomposite films with antimicrobial activity. J Agric Food Chem 54, 5814-5822. **DOI**:10.1021/jf060658h

[18] Wawrzyńczak A, Jarmolińska S, Nowak I; (2022) Nanostructured KIT-6 materials functionalized with sulfonic groups for catalytic purposes. Catal Today 397-399, 526-539. **DOI**:10.1016/j.cattod.2021.06.019

[19] Feliczak-Guzik A, Jadach B, Piotrowska H, Murias M, Lulek J, Nowak I; (2016) Synthesis and characterization of SBA-16 type mesoporous materials containing amine groups. Microporous Mesoporous Mater 220, 231-238. **DOI**:10.1016/j.micromeso.2015.09.006

[20] Thommes M, Kaneko K, Neimark AV, Olivier JP, Rodriguez-Reinoso F, Rouquerol J, Sing KSW; (2015) Physisorption of gases, with special reference to the evaluation of surface area and pore size distribution (IUPAC Technical Report). Pure Appl Chem 87, 1051-1069. **DOI**:10.1515/pac-2014-1117

[21] Prouzet E, Pinnavaia TJ; (1997) Assembly of mesoporous molecular sieves containing wormhole motifs by a nonionic surfactant pathway: control of pore size by synthesis temperature. Angew Chem Int Ed 36, 516-518. **DOI**:10.1002/anie.199705161

[22] Nowak I, Kilos B, Ziolek M, Lewandowska A; (2003) Epoxidation of cyclohexene on Nb-containing meso- and macroporous materials. Catal Today 78, 487-498. **DOI**:10.1016/S0920-5861(02)00332-2

[23] Feliczak-Guzik A, Sprynskyy M, Nowak I, Jaroniec M, Buszewski B; (2018) Application of novel hierarchical niobium-containing zeolites for the synthesis of alkyl lactate and lactic acid. J Colloid Interf Sci 516, 379-383. **DOI**:10.1016/j.jcis.2018.01.090

[24] Nowak I, Ziolek M, Jaroniec M (2004) Synthesis and characterization of polymer-templated mesoporous silicas containing niobium. J Phys Chem B 108, 12, 3722-3727. **DOI**:10.1021/jp036978a

[25] Nowak I, Feliczak A, Nekosova I, Cejka; (2007) Comparison of oxidation properties of Nb and Sn in mesoporous molecular sieves. J Appl Catal A General 321, 40. **DOI**:10.1016/j.apcata.2007.01.025

[26] Djelad A, Morsli A, Robitzer M, Bengueddach A, Di Renzo F, Quignard F; (2016) Sorption of Cu(II) ions on chitosan-zeolite x composites: impact of gelling and drying conditions. Molecules 21, 109-124. **DOI**:10.3390/molecules21010109

[27] Gao Y, Ru Y, Zhou L, Wang X, Wang J; (2018) Preparation and characterization of chitosan-zeolite molecular sieve composite for ammonia and nitrate removal. Adv Compos Lett 27(5), 185-192. **DOI**:10.1177/096369351802700502